Neuronal necrosis is regulated by a conserved chromatin-modifying cascade

Kai Liu[a], Lianggong Ding[a], Yuhong Li[a,b], Hui Yang[a], Chunyue Zhao[a], Ye Lei[a], Shuting Han[a], Wei Tao[c], Dengshun Miao[d], Hermann Steller[e], Michael J. Welsh[b,1], and Lei Liu[a,f,1]

[a]The State Key Laboratory of Biomembrane and Membrane Biotechnology, School of Life Sciences, Peking University, Beijing 100871, China; [b]Howard Hughes Medical Institute, Department of Internal Medicine, University of Iowa, Iowa City, IA 52242; [c]The Education Ministry Key Laboratory of Cell Proliferation and Differentiation, School of Life Sciences, Peking University, Beijing 100871, China; [d]State Key Laboratory of Reproductive Medicine, Research Center for Bone and Stem Cells, Department of Anatomy, Nanjing Medical University, Nanjing, Jiangsu 210029 China; [e]Howard Hughes Medical Institute, Strang Laboratory of Apoptosis and Cancer Biology, The Rockefeller University, New York, NY 10065; and [f]Beijing Institute for Brain Disorders, Department of Neurobiology, Capital Medical University, Youanmen, Beijing 100069, China

Contributed by Michael J. Welsh, August 5, 2014 (sent for review May 21, 2014)

Neuronal necrosis induced by calcium overload causes devastating brain dysfunction in diseases such as stroke and brain trauma. It has been considered a stochastic event lacking genetic regulation, and pharmacological means to suppress neuronal necrosis are lacking. Using a *Drosophila* model of calcium overloading, we found JIL-1/mitogen- and stress-activated protein kinase 1/2 is a regulator of neuronal necrosis through phosphorylation of histone H3 serine 28 (H3S28ph). Further, we identified its downstream events including displacement of polycomb repressive complex 1 (PRC1) and activation of Trithorax (Trx). To test the role of JIL-1/PRC1/Trx cascade in mammals, we studied the necrosis induced by glutamate in rat cortical neuron cultures and rodent models of brain ischemia and found the cascade is activated in these conditions and inhibition of the cascade suppresses necrosis in vitro and in vivo. Together, our research demonstrates that neuronal necrosis is regulated by a chromatin-modifying cascade, and this discovery may provide potential therapeutic targets and biomarkers for neuronal necrosis.

neurodegeneration | epigenetics | histone modification | H3K4me3 | aging

Glutamate-induced neuronal necrosis has been implicated in many devastating neurodegenerative diseases, including stroke, traumatic brain injury, epilepsy, and Alzheimer's disease (1, 2). Ischemic stroke, for instance, is caused by a lack of oxygen and glucose in the brain, which leads to the excessive accumulation of glutamate in the extracellular space. Glutamate then activates *N*-methyl-D-aspartate (NMDA) receptors, which trigger calcium influx and a series of detrimental events, including production of nitric oxide (NO), activation of extracellular signal-regulated kinase (ERK1/2) and calpain, swelling of organelles, rupture of plasma membrane, and irreversible necrotic cell death in neurons (1, 3, 4). Calcium overload can activate the ERK pathway (5), and the translocation of activated ERK1/2 into the nucleus is required for their detrimental effect in neuronal necrosis (6), suggesting an unknown target in the nucleus may play a crucial role. In addition, chromatin modifications have been reported to associate with many pathological conditions of neurodegeneration (7). However, the molecular mechanism of chromatin alternations and their functional role remain to be investigated (8, 9).

Previously, gain-of-function (GOF) mutants of the degenerin/epithelial Na^+ channel (DEG/ENaC) family (*deg-1* and *mec-4*) or of the acetylcholine receptor subunit *gsa-1* (which results in the constitutive opening of these cation channels) were found to induce chronic neuronal necrosis in *Caenorhabditis elegans* (10, 11). However, genetic models of transient calcium overload are lacking, which hinders our understanding of the initial cellular responses to necrotic insults. Here, we describe the generation of a *Drosophila* model of transient necrosis and its application in studying the molecular mechanisms of neuronal necrosis. We discovered that necrosis was regulated by a chromatin-modifying cascade. Importantly, this regulatory mechanism was conserved in mammalian neuronal necrosis.

Results

A Transient Model of Neuronal Necrosis in *Drosophila*. To mimic calcium overload, we generated a transgenic fly line expressing the rat glutamate receptor 1 Lurcher mutant (*UAS-GluR1^{Lc}*), a constitutively open channel with high permeability to calcium (12). Previously, we confirmed that the constitutive expression of this leaky channel resulted in neuronal necrosis in *Drosophila* photoreceptor cells (13). To temporally control the expression of *GluR1^{Lc}* in neurons, we combined a panneuronal promoter *Appl-Gal4* with *tubulin-Gal80^{ts}*, a temperature-sensitive inhibitor protein of Gal4 (*Appl > GluR1^{Lc}*; *tubulin-Gal80^{ts}* line is simplified as *AG*). At the permissive temperature (18 °C), these flies did not express *GluR1^{Lc}* and developed normally. When the flies were transferred to the restrictive temperature (30 °C), Gal80^{ts} lost its function and *GluR1^{Lc}* expression was initiated. To study the morphological changes of neurons, *UAS-GFP* was included (*Appl > GluR1^{Lc}/GFP*; *tubulin-Gal80^{ts}* line is simplified to *AGG*). We examined the larval chordotonal neurons (Ch N) because of their stereotypic morphology. After incubation at 30 °C for 18 h, Ch N displayed progressive defects, including swollen soma and dendritic segments, loss of regular cell shape, and release of GFP to the extracellular space, suggesting the integrity of plasma membrane was compromised (Fig. 1*A*). These features are consistent with the characters of classical necrosis (1). To further verify the nature of cell death, the larval ventral nerve cord (VNC) of *AG* flies were stained with

Significance

Neuronal necrosis widely occurs in devastating neurodegenerative diseases, such as stroke, traumatic brain injury, and Alzheimer's disease. However, it has long been considered a stochastic process lacking genetic regulations. Our inadequate understanding of its molecular mechanism has hindered pharmacological design to suppress this type of cell death. Through construction and studying of a *Drosophila* model of neuronal necrosis, we identified a chromatin-modifying cascade to play a key role in execution of neuronal necrosis. Our results indicate that neuronal necrosis is a stereotypically regulated process in both insect and mammalian neurons. This discovery provides previously unidentified biomarkers and potential therapeutic targets for neuronal necrosis.

Author contributions: K.L., M.J.W., and L.L. designed research; K.L., L.D., Y. Li, H.Y., C.Z., Y. Lei, and S.H. performed research; K.L., W.T., D.M., H.S., M.J.W., and L.L. analyzed data; and K.L., M.J.W., and L.L. wrote the paper.

The authors declare no conflict of interest.

Freely available online through the PNAS open access option.

[1]To whom correspondence may be addressed. Email: michael-welsh@uiowa.edu or leiliu@pku.edu.cn.

This article contains supporting information online at www.pnas.org/lookup/suppl/doi:10.1073/pnas.1413644111/-/DCSupplemental.

www.pnas.org/cgi/doi/10.1073/pnas.1413644111

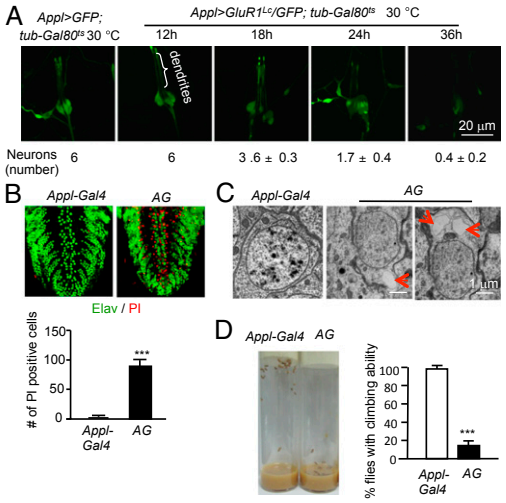

Fig. 1. Characterization of the *AG* model of neuronal necrosis. (*A*) Morphological changes of Ch N after the induction of necrosis in *AGG* flies. The average number of Ch N in one chordotonal organ is shown for each time point. $n = 25$ chordotonal organs from five larvae. (*B*) Immunofluorescent staining of larval VNCs with anti-Elav (a neuron marker) and PI. Of note, Elav was not colocalized with PI. Immunofluorescent staining with PI and anti-Repo (a glial cell marker) showed that they did not colocalize either (Fig. S1*A*). Because the number of neurons but not glial cells was reduced, the PI-positive cells were likely neurons that had lost Elav staining. Quantification of PI positive neurons is shown as mean + SD. $n = 6$ larval VNCs. $P < 0.001$. For all figures, open bars indicate controls; gray bars indicate that there was no difference between treated groups and controls; black bars indicate a statistically significant difference. $*P < 0.05$; $**P < 0.01$; $***P < 0.001$ throughout the figures. (*C*) TEM images of the protocerebrum region in the adult fly brain. *Appl-Gal4* is shown as the wild-type control. Neurons in the *AG* brains displayed large vacuoles (red arrows). $n = 10$ slides. (*D*) Example of the climbing tube assay. Quantification of flies that were able to climb up a tube is presented as mean + SD. $n = 4$ trials. $P < 0.001$.

propidium iodide (PI), a cell-impermeable dye. The induction of $GluR1^{Lc}$ expression resulted in ~80 PI-positive neurons in each VNC before fly death (Fig. 1*B* and Fig. S1*A*), indicating the integrity of neuron plasma membrane in *AG* flies was disrupted. Moreover, about 1% neurons in the adult *AG* fly brains displayed intracellular vacuoles, another marker for necrotic cell death (Fig. 1*C*) (10, 14). Together, these results indicated that the nature of cell death in *AG* flies was necrotic. To quantify the functional consequence of neuronal necrosis, the adult *AG* flies were incubated at 30 °C for 12 h and then transferred back to 18 °C. After 48 h, less than 20% of them were able to climb up tubes (Fig. 1*D*), suggesting that the transient expression of $GluR1^{Lc}$ caused dysfunction of the nervous system.

JIL-1 Is a Novel Regulator of Neuronal Necrosis in *Drosophila*. Using the *AG* climbing tube defect model, we performed a genetic screen on protein kinases, which have been proved to play important roles in necroptosis (15). The *Drosophila* genome encodes 313 known and predicted kinases (16, 17). We obtained 289 available mutant lines covering 222 kinase genes (Dataset S1). By far, we have tested 42 lines and found heterozygous mutants of 7 kinases had rescue effect (Dataset S2). We focused on JIL-1, the *Drosophila* homolog of mitogen- and stress-activated protein kinase 1/2 (MSK1/2), because it is a histone kinase and regulates chromatin remodeling (18). Chromatin modifications are associated with many neurodegenerative conditions; however, their functional importance and molecular mechanism in neurodegeneration are largely unknown (7). The mutations of *JIL-1* ($JIL\text{-}1^3$ and $JIL\text{-}1^{z2}$) were able to rescue the climbing ability of *AG* flies (Fig. 2*A*) and suppress neuronal necrosis in the *AGG* model (Fig. 2*B*), and did not affect the protein level of $GluR1^{Lc}$ (Fig. S1*B*). $JIL\text{-}1^3$ is a mutant of JIL-1 with C-terminal 166 amino acids truncated, and $JIL\text{-}1^{z2}$ is a null allele (18, 19).

Recently, it has been demonstrated that MSK1/2 and JIL-1 can phosphorylate histone H3 serine 28 (H3S28ph) (20, 21). Therefore, we assessed the level of H3S28ph and found that it was increased in the larval VNC of the *AG* flies (Fig. 2*C*). The Western blot analysis further confirmed the increase of H3S28ph levels in the adult *AG* brains (Fig. 2*D*). These results suggested that the JIL-1 activity was increased in neuronal necrosis.

Downstream of JIL-1 Function Is PRC1 Loss and Trx Activation. JIL-1/MSK1/2-mediated H3S28ph can displace Polycomb repressive complex 1 (PRC1) from chromatin and activates gene expression (20, 21). Therefore, PRC1 loss of function (LOF) may be the downstream event of JIL-1-mediated H3S28ph in necrosis. Consistently, we found that mutations of *Polycomb* (*Pc*, including Pc^1 and Pc^{f01890}), a core component of PRC1, enhanced necrosis in the *AGG* model (Fig. 3*A*). As controls, these mutants indeed reduced the protein level of Pc (Fig. S1*C*) and did not affect the development of the Ch N (Fig. S1*D*). Moreover, we found that Pc^{f01890} suppressed the rescue effect of $JIL\text{-}1^3$ in the *AGG* model (Fig. 3*B*), indicating PRC1 functioned downstream of JIL-1 in neuronal necrosis.

PRC1 and Trithorax (Trx) counteract with each other to regulate transcription (22, 23). Generation of H3K4me3, a histone modification normally associated with active transcriptional loci, is the primary mechanism by which Trx regulates chromatin structure and gene expression (22). Therefore, H3S28ph-mediated PRC1 loss may disinhibit Trx in neuronal necrosis. Indeed, the level of H3K4me3 was elevated in the Ch N of the *AGG* flies, suggesting Trx was activated (Fig. 3*C*). To test the functional role

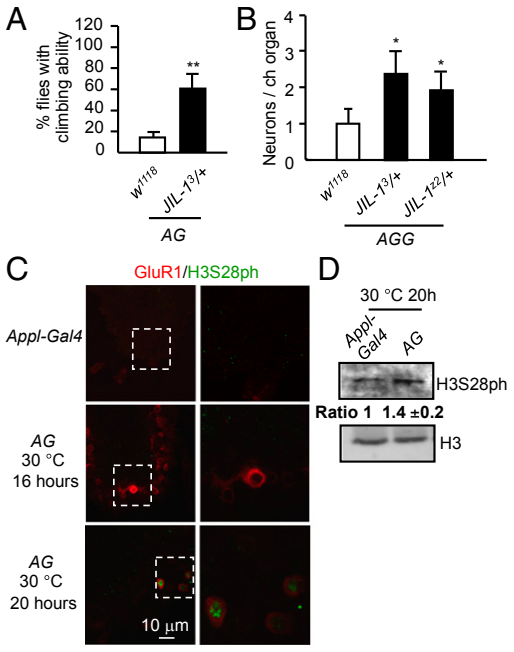

Fig. 2. The function of JIL-1 on neuronal necrosis in the *AG* flies. (*A*) Quantification of the climbing tube assay using the *AG* model. Data are presented as mean + SD. $n = 4$ trials. $P = 0.004$. (*B*) *JIL-1* mutations suppressed neuronal necrosis in *AGG* flies. Mean + SD. $n = 25$ chordotonal organs from five larvae. $P = 0.014$ for $JIL\text{-}1^3$; $P = 0.028$ for $JIL\text{-}1^{z2}$. (*C*) Immunostaining of H3S28ph in the larval VNCs. The result reveals that H3S28ph was increased in about 1% of neurons in the *AG* flies after incubation at 30 °C for 20 h. $n = 3$ trials. (*D*) Western blot of nuclear extracts from adult *AG* fly heads after incubation at 30 °C for 20 h. H3 is the loading control. $n = 2$ trials.

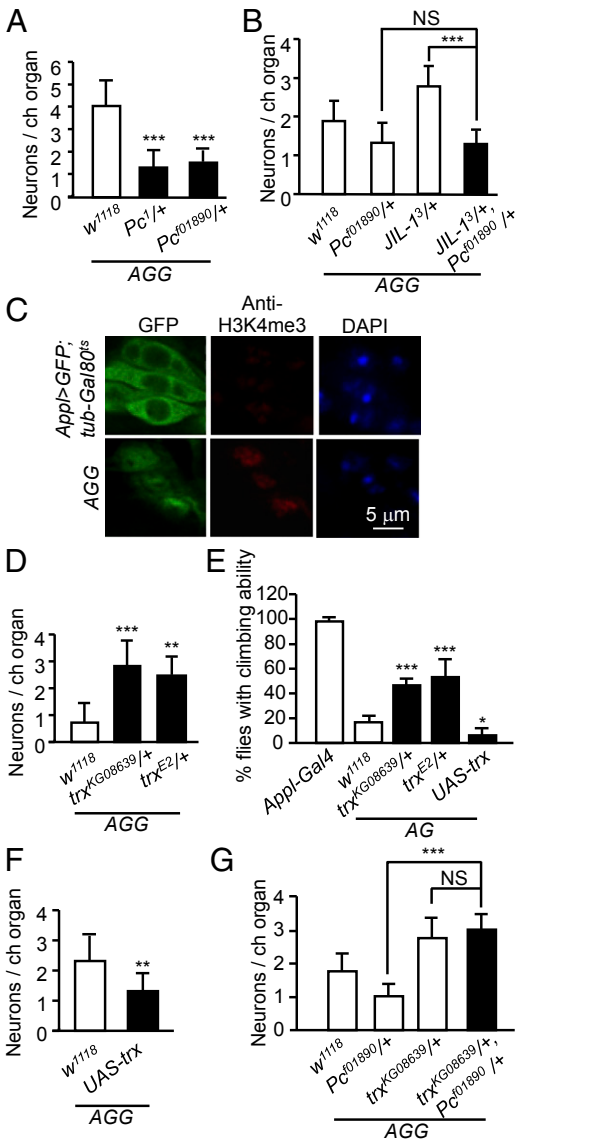

Fig. 3. PRC1 and Trx function downstream of JIL-1 in the *AG* flies. (*A*) *Pc* mutations enhanced neuronal necrosis in *AGG* flies. Mean + SD. $n = 25$ chordotonal organs from five larvae. $P < 0.001$ for both mutants. (*B*) Genetic interaction between *JIL-1* and *Pc* in *AGG* flies. Mean + SD. $n = 25$ chordotonal organs from five larvae. $P = 0.789$ for Pc^{f01890} vs. $JIL\text{-}1^{3}$, Pc^{f01890}; $P < 0.001$ for $JIL\text{-}1^{3}$ vs. $JIL\text{-}1^{3}$, Pc^{f01890}. (*C*) Immunofluorescent staining of the Ch N. The staining intensity of H3K4me3 was higher in *AGG* flies than in the control flies (*Appl > GFP; tub-Gal80^{ts}*). $n = 2$ trials, six chordotonal organs were examined in each trial. (*D*) *Trx* mutations suppressed neuronal necrosis in *AGG* flies. Mean + SD. $n = 25$ chordotonal organs from five larvae. $P < 0.001$ for $trx^{KG08639}$; $P = 0.002$ for trx^{E2}. (*E*) Effect of LOF and GOF of *trx* on the climbing ability of the *AG* flies. Mean + SD. $n = 4, 8, 4, 4$, and 7 trials. $P < 0.001$ for $trx^{KG08639}$ and trx^{E2}; $P = 0.021$ for *UAS-trx*. (*F*) GOF *trx* enhanced neuronal necrosis in *AGG* flies. Mean + SD. $n = 25$ chordotonal organs from five larvae. $P = 0.002$. (*G*) Genetic interaction between *trx* and *Pc* in the *AGG* flies. Mean + SD. $n = 25$ chordotonal organs from five larvae. $P < 0.001$ for Pc^{f01890} vs. $trx^{KG08639}$, Pc^{f01890}; $P = 0.819$ for $trx^{KG08639}$ vs. $trx^{KG08639}$, Pc^{f01890}.

of Trx, we studied two mutants, trx^{E2} (an amorphic allele) (24) and $trx^{KG08639}$ (a P-element insertion mutant). The disruption of *trx* transcripts in the $trx^{KG08639}$ flies was verified by RT-qPCR (Fig. S1*E*). Strikingly, these mutants suppressed the necrosis of the Ch N and climbing defect of *AG* flies (Fig. 3 *D* and *E*). Consistently, overexpression of *trx* enhanced necrosis (Fig. 3 *E* and *F*). As a transcriptional activator, *trx* may affect the transcription of $GluR1^{Lc}$. However, the protein level of $GluR1^{Lc}$ was unaltered under the *trx* LOF or GOF background (Fig. S1*F*). Moreover, $trx^{KG08639}$ was capable of suppressing the effect of Pc^{f01890} on necrosis (Fig. 3*G*), indicating Trx functioned downstream of Pc. Together, these results indicated that Trx promoted neuronal necrosis downstream of PRC1.

We also investigated the effect of *JIL-1*, *Pc*, and *trx* mutants on apoptosis and found none of them affected apoptosis (Fig. S1*G*), suggesting the function of JIL-1/PRC1/Trx was specific to necrosis.

The JIL-1/PRC1/Trx Cascade in Mammalian Neuronal Necrosis. To evaluate the conservation of JIL-1/PRC1/Trx cascade in mammals, we investigated glutamate-induced cell death in rat cortical neuron cultures. First, we confirmed that ~95% of cells died by calpain-mediated necrosis but not RIP1-mediated necroptosis (25) [Fig. S2, note that the lactate dehydrogenase (LDH) release index is a more quantitative measurement of cell death than the PI staining counts; however, its change was less dramatic because some LDH was not released by the dead cells]. We then determined the level of H3S28ph, and found that it was elevated after glutamate treatment (Fig. 4*A*), whereas the levels of other histone modifications (H3K27me3, H3K9ac, and H4K12ac) were unaltered (Fig. 4*A*).

The increase of H3S28ph suggests the activation of MSK1/2. Consistently, we found that the level of active MSK1/2 (MSK1/2 phosphorylated on Thr581) was increased after glutamate treatment (Fig. 4*B*). In addition, we observed that the increase of H3S28ph and the activation of MSK1/2 occurred in the same neurons (Fig. 4*B*), supporting a causal relationship between them. To directly test the role of MSK1/2 in phosphorylation of H3S28, we applied an inhibitor of MSK1/2, H89 and found it suppressed the elevation of H3S28ph levels in necrosis; in contrast, neither a calpain inhibitor (MDL-28170) nor a caspase inhibitor (z-VAD) had any effect (Fig. 4*C*). H89 is also an inhibitor of cAMP-dependent protein kinase (PKA) (26). To distinguish the role of PKA from that of MSK1/2, we examined PKI, a specific inhibitor of PKA (26). The result revealed that PKI had no effect on the production of H3S28ph (Fig. 4*C*). Together, these results indicated that MSK1/2 were the enzymes phosphorylating H3S28, and the activation of JIL-1/MSK1/2 was a conserved process in *Drosophila* and mammalian neuronal necrosis.

To examine the events upstream of MSK1/2 activation, we first evaluated the role of the NMDA receptor, and found that MK-801, a NMDA receptor blocker, inhibited the increase of H3S28ph (Fig. S3*A*). Next, we examined two kinases, ERK1/2 and p38, the direct upstream activators of MSK1/2 (27, 28). We found that PD184352, an inhibitor of ERK1/2 activation, inhibited the increase of H3S28ph (Fig. 4*D* and Fig. S3*B*). However, SB203580, an inhibitor of p38α/β, had no effect (Fig. 4*D*). Furthermore, the active ERK1/2 level was elevated after glutamate treatment (Fig. S3*C*), and PD184352 suppressed neuronal necrosis (Fig. S3*D*). These results were consistent with previous reports (4) and suggested that ERK1/2 were likely the kinases that activated MSK1/2 in neuronal necrosis.

PRC1 can ubiquitinate histone H2A to generate H2A monoubiquitination (ubH2A) (29). We found ubH2A levels declined after glutamate treatment (Fig. 4*A*), suggesting loss of PRC1 function in necrotic neurons. Consistently, the immunofluorescence data revealed that the intensity of Bmi-1, a core component of PRC1, was reduced in the nucleus (Fig. 4*E*). However, its protein level was unaltered (Fig. S4*A*), suggesting displacement of Bmi-1 from chromatin, instead of degradation. Interestingly, the displacement of Bmi-1 was suppressed by H89, suggesting MSK1/2 were likely responsible for the change of PRC1 (Fig. 4*E*).

To study the role of Trx-mediated H3K4me3 in mammalian neuronal necrosis, we performed immunofluorescence assay, and

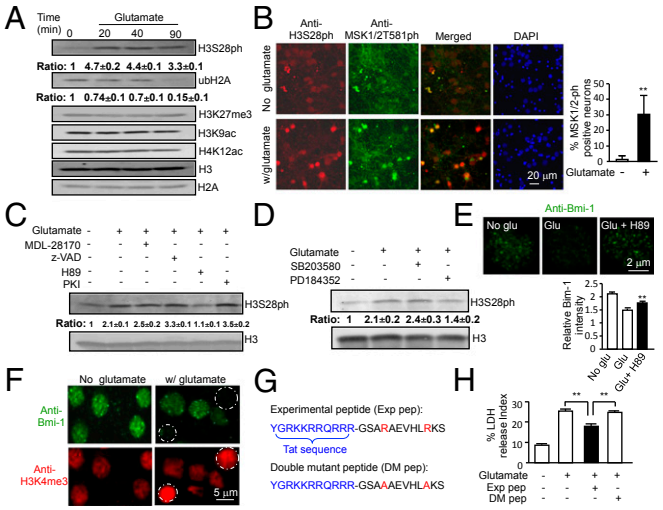

Fig. 4. Chromatin regulation of necrosis in mammalian neurons. (*A*) Western blot of nuclear extracts from glutamate-treated neuron cultures. The time points of the sample collection are indicated above the *Top* panel. H3 and H2A are the loading controls. $n = 3$ trials. (*B*) Immunofluorescent staining of H3S28ph and the active form of MSK1/2 (MSK1/2T581ph). DAPI was used to label nuclei. The percentage of MSK1/2T581ph-positive neurons is presented as mean + SD. $n = 3$ trials. $P = 0.003$. (*C*) The effect of several drugs on H3S28ph levels based on Western blot. The following drug concentrations were used: MDL-28170, 200 μM; z-VAD, 100 μM; H89, 20 μM; and PKI, 20 μM. The neuron cultures were pretreated with the indicated drug for 1 h before glutamate treatment for 30 min. H3 is the loading control. $n = 2$ trials. (*D*) The effect of PD184352 and SB203580 on H3S28ph production. The drug concentrations were PD184352, 10 μM and SB203580, 30 μM. The treatment procedure was the same as in *C*. H3, loading control. $n = 2$ trials. (*E*) The immunofluorescent staining of anti–Bmi-1. The treatment procedure was the same as in *C*. Quantification of the staining intensity in individual cells is shown as mean + SD. $n = 32$, 39, and 32 cells. $P < 0.001$ for no glutamate vs. glutamate; $P = 0.002$ for glutamate + H89 vs. glutamate. (*F*) Immunofluorescent staining of anti–Bmi-1 and anti-H3K4me3 after glutamate treatment for 30 min. Bmi-1 displacement and increased levels of H3K4me3 were observed in the same neurons (white circles). $n = 3$ trials. (*G*) The amino acid sequences of the Exp pep and DM pep. The blue letters indicate the cell-penetrating sequence of the HIV-1 Tat protein. The red letters indicate the critical arginine residues in the Exp pep that are mutated to alanine in the DM pep. (*H*) The LDH release assay reveals that the Exp pep (but not the DM pep) reduced neuronal necrosis. The neuron cultures were pretreated with 4 μM of the Exp pep or the DM pep for 1 h and then treated with 200 μM glutamate for 4 h. Mean + SEM. $n = 3$ trials. $P = 0.005$ for no peptide vs. Exp pep, $P = 0.003$ for DM pep vs. Exp pep.

found that H3K4me3 intensity was increased by 29% in neurons with reduced Bmi-1 intensity after glutamate treatment (Fig. 4*F* and Fig. S4*B*). To evaluate the functional importance of Trx in mammalian neurons, we designed a shRNA to knock down the expression of WDR5 (Fig. S4*C*), a core component of Trx/MLL (the homolog of *Drosophila* Trx) complexes (30). We found that WDR5 shRNA delivered via lentivirus partially suppressed neuronal necrosis (Fig. S4*D*). The limited effectiveness of this shRNA was likely because transient knockdown of WDR5 transcripts might not extensively reduce the WDR5 protein level. Indeed, the result of Western blot indicated that the protein level of WDR5 was only reduced 17% (Fig. S4*E*). To target WDR5 protein function directly, we synthesized a small peptide. This peptide mimics the interaction motif of MLL1 with WDR5 and has been demonstrated to interfere with the assembly of the Trx/MLL complex in vitro (31). To render this peptide permeable to cells, the cell membrane transduction domain of HIV-1 Tat protein (YGRKKRRQRRR) was added to the N terminus of the peptide, called experimental peptide (Exp pep, Fig. 4*G*). As a control of the peptide, we mutated two essential arginine residues to alanine, called double-mutant peptide (DM pep, Fig. 4*G*). First, we validated the interference of the Exp pep with the WDR5–MLL1 interaction via coimmunoprecipitation (Fig. S4*F*). Then, we confirmed that the Exp pep inhibited the increased production of H3K4me3 after glutamate treatment (Fig. S4*G*), without affecting Bmi-1 loss (Fig. S4*H*). Next, we investigated the effect of the Exp pep on necrosis and discovered that it suppressed cell death in glutamate-treated neuron cultures (Fig. 4*H*).

To determine whether the suppressed cell death was necrotic in nature, we examined chromatin morphology via DAPI staining. Nuclei displaying small and irregular chromatin clumps are characteristic of necrosis; whereas nuclei displaying large and round chromatin clumps are characteristic of apoptosis (32). We found that the Exp pep reduced the proportion of neurons displaying necrotic chromatin morphology (Fig. S4*I*). The conclusion was further supported by costaining with PI and Annexin V (Fig. S4*J*). Collectively, our results demonstrated that interfering with the activity of the Trx/MLL complex inhibited neuronal necrosis.

Calpain is a crucial mediator of neuronal necrosis. To clarify the relationship between calpain and JIL-1/PRC1/Trx cascade, we examined the time course of calpain activation and the increase of H3S28ph in necrotic cells. Calpain activation was measured based on its cleavage of p35. The result demonstrated that both cleavage of p35 and the increase in H3S28ph production occurred as early as 5 min after glutamate treatment (Fig. S5*A*). This result was consistent with Fig. 4*C*, showing that the calpain inhibitor MDL-28170 did not affect the increase of H3S28ph. Furthermore, the Exp pep did not alter the calpain-mediated cleavage of p35 (Fig. S5*B*) or calcium influx (Fig. S5*C*). Together, these results indicated that the JIL-1/PRC1/Trx cascade functioned in parallel with the calpain activation.

The JIL-1/PRC1/Trx Cascade in Rodent Models of Ischemic Stroke. Neuronal necrosis predominantly occurs in the ischemic core of the stroke brains (3). To determine whether the JIL-1/PRC1/Trx cascade is activated during stroke, we studied the transient global ischemia/reperfusion model in mice (33). In the nuclear proteins collected from the hippocampus, we detected increased H3S28ph and decreased ubH2A levels as early as 1 h after the onset of ischemia, whereas other histone modifications (H3K27me3, H3K9ac, and H4K12ac) were not altered (Fig. 5*A*). To explore the functional role of Trx, we administered the Exp pep via tail vein injection. However, these mice exhibited reduced activity, likely due to the regulation of globin gene expression by WDR5 (34), which may reduce the oxygen transport of hemoglobin. To reduce the side effect, we delivered the peptides directly into the lateral ventricle of the mouse brains. Result from triphenyl-tetrazolium chloride (TTC) staining, which detects dysfunctional mitochondria in brain sections, indicated that the Exp pep significantly reduced the infarct volume compared with the DM pep (Fig. 5*B*).

The permanent occlusion model in rats is more commonly used for stroke research. Therefore, we also examined unilateral middle cerebral artery occlusion (MCAO) in rats. Different from the results of the mouse ischemic stroke model, the increase of H3S28ph was not detectable by Western blot, likely due to the unsynchronized death of neurons in the brain. Indeed, the result of immunofluorescence assay showed that ~27% of the neurons displayed increased H3S28ph intensity (Fig. S5*D*). Consistent with the mouse data, the Exp pep significantly reduced the infarct volumes upon delivery into the lateral ventricle (Fig. 5*C*). Altogether, our results indicate that the JIL-1/PRC1/Trx cascade was activated in rodent models of stroke and blocking the cascade alleviated brain damage.

Discussion

Modeling Calcium Overload in *Drosophila* Reveals a Conserved Chromatin-Modifying Cascade That Mediates Necrosis. Neuronal necrosis is predominantly caused by hyperactivation of NMDA

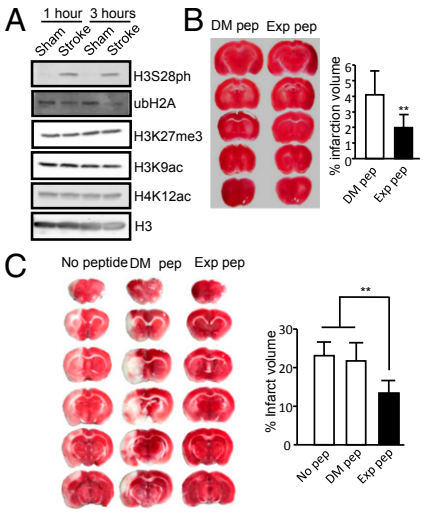

Fig. 5. The JIL-1/PRC1/Trx cascade in rodent ischemic stroke models. (*A*) Western blot of nuclear extracts from the hippocampal region of the mouse global ischemia/reperfusion model. The time points of sample collection after ischemia are shown above the *Top* panel. H3, loading control. $n = 2$ trials. (*B*) TTC staining image displaying the brain damage in the mouse global ischemia/reperfusion model. The quantitative data are presented as mean + SD. $n = 11$ and 9 mice. $P = 0.002$. (*C*) TTC staining image displaying the brain damage in the rat MCAO model. The quantitative data are presented as mean + SD. $n = 5$, 7, and 7 rats. $P = 0.001$ for no peptide vs. Exp pep, $P = 0.002$ for DM pep vs. Exp pep.

receptors and excessive calcium influx; these processes stimulate diverse detrimental events, including the activation of calpains and ERK1/2 (4, 35). However, our understanding of the signaling events downstream of calcium overload remains inadequate. Through the temporally regulated expression of a leaky channel, we established a model of transient calcium overload in *Drosophila*. Our genetic studies identified a chromatin-modifying cascade that regulated necrosis. This cascade was conserved from insects to mammals. Our experimental data suggest the following model (Fig. 6). Initially, the massive calcium influx activated the ERK1/2 pathway. Next, ERK1/2 stimulated MSK1/2, which, in turn, increased H3S28ph. The increased levels of H3S28ph promoted the displacement of PRC1. The loss of PRC1 activated Trx and led to neuronal necrosis. Our results also suggested that specific alterations of histone modifications occurred in necrosis, including increased levels of H3S28ph and H3K4me3, and decreased levels of ubH2A. They may serve as novel markers of neuronal necrosis.

The downstream of the JIL-1/PRC1/Trx cascade is likely the regulation of transcription. In support of this possibility, SREBP-1, a transcription factor, is activated upon calcium overload and regulates calpain-dependent neuronal cell death (36). Conversely, it has been reported that RNA polymerase II inhibitor (actinomycin D) and protein translation inhibitor (cycloheximide) cannot rescue glutamate-induced cell death in neuron cultures (37), suggesting that mRNA transcription and protein synthesis may not be involved in necrosis execution. However, residual activity of RNA polymerase II or ribosome may still function after the drug blockage. The roles of mRNA transcription and protein synthesis in necrosis require further investigation.

The JIL-1/PRC1/Trx Cascade Functions Downstream of ERK1/2 and in Parallel with Calpain. ERK1/2 have been reported to promote caspase-independent nonapoptotic neuronal death in vivo and in vitro (4, 38), and the translocation of activated ERK1/2 into the nucleus is essential for their detrimental role (6). However, the downstream activities of ERK1/2 in the nucleus are unclear (4). Our results revealed that the increase of H3S28ph levels in neuronal necrosis was blocked by PD184352, an inhibitor of ERK1/2 activation. Therefore, the nuclear target of ERK1/2 is likely the JIL-1/PRC1/Trx cascade. Interestingly, the ERK–MSK1 pathway has been reported to phosphorylate ataxin 1 and promote neurodegeneration in spinocerebellar ataxia type 1 disease (SCA1) (39). Together with our study, it implies that the ERK–MSK1/2 pathway may have a general role in neuronal-death–related diseases. It also suggests a new linkage between necrosis and neurodegenerative diseases. In addition, we propose that the JIL-1/PRC1/Trx cascade functioned in parallel with calpain, as the calpain inhibitor MDL-28170 did not affect H3S28ph production and the blockage of Trx with the Exp pep did not alter calpain-mediated p35 cleavage. Calcium overload and calpain activation have been considered to cause irreversible damage to neurons (35, 40). However, our data indicated that it was likely not the case, because neurons could survive from these stresses upon inhibition of the Trx function.

Role of PRC1 in Aging. Our research demonstrated that loss of PRC1 promoted neuronal necrosis in *Drosophila*, indicating PRC1 might protect neurons from necrosis. A previous study shows that Bmi-1 is down-regulated in aged mouse brain (41). This implies that older people may suffer more severe neuronal necrosis after vascular occlusion. Consistently, a study in mice indicates that aging aggravates ischemic-stroke–induced brain damage (42).

Chromatin-Modifying Enzymes as Potential Therapeutic Targets for Neuronal Necrosis. NMDA receptor-mediated glutamate excitotoxicity is a predominant cause of neuronal death in many neurodegenerative diseases (43); however, the clinical trials of antagonists of NMDA receptors have not been promising due to their side effects (44). Recent studies suggest that targeting of downstream events of NMDA receptors is likely to be an effective approach (36, 45). Our study suggested that the JIL-1/PRC1/Trx cascade, which functioned downstream of the NMDA receptors, might represent a set of drug targets independent from calpain activation. Targeting of this cascade has several advantages. First, its action was dominant, because the heterozygous mutants of this pathway were sufficient to suppress neuronal necrosis; as a result, pharmacological targeting may be easier to achieve. In addition, inhibition of this pathway exhibited low toxicity, because the heterozygous mutant flies developed normally. Although the systemic delivery of the Exp pep was not successful, likely due to functions of WDR5 beyond neurons, targeting other proteins in the cascade may resolve this problem.

Materials and Methods

Fly Maintenance and Stocks. Flies were raised on standard sucrose/cornmeal medium at constant 18 °C or 25 °C with a 12-h light and 12-h dark cycle. All

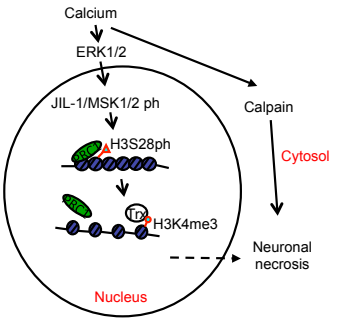

Fig. 6. Model depicting the regulation of neuronal necrosis by the JIL-1/PRC1/Trx cascade. Calcium influx activates the ERK1/2. ERK1/2 activate MSK1/2 /JIL-1, which increases H3S28 phosphorylation. The increased levels of H3S28ph displace PRC1 from chromatin. The loss of PRC1 from chromatin activates Trx, which leads to increased levels of H3K4me3. Then, it results in neuronal necrosis by an unknown mechanism. This cascade functions in parallel with the calpain activation.

fly lines were obtained from the Bloomington *Drosophila* Stock Center, except *JIL-1*^{z2} (Kristen Johansen, Iowa State University, Ames, IA).

Genetic Screening. The AG flies were crossed with point mutations or P-element–based mutations obtained from the Bloomington *Drosophila* Stock Center, and raised at 18 °C. The 3-d-old progeny flies were incubated at 30 °C for 12 h and then transferred back to 18 °C. After 48 h, the climbing ability of the flies was assessed. The flies that were able to reach the top of a 10-cm tube within 30 s were defined as the ones with climbing ability.

Rodent Ischemia Models. All experiments were approved by the Institutional Animal Care and Use Committee, Peking University. For the mouse ischemia/reperfusion model, we used 8-week-old C57BL/6 male mice (17–20 g, Department of Laboratory Animal Science, Peking University Health Science Center), housed with a 12-h light and 12-h dark cycle. The method for ischemia/reperfusion followed a previous protocol (33). We injected 0.7 μg of the Exp pep or DM pep in 4 μL saline into the lateral ventricle of the mouse immediately before the ischemia surgery, and infarct volume was determined 5 d later. We excluded two mice that died within 5 d due to failure of surgery. For the rat MCAO model, we used adult male Sprague-Dawley rats (250–270 g), housed with a 12-h light and 12-h dark cycle. The permanent MCAO method followed previous protocols (46, 47). A laser Doppler blood flow monitor was used to ensure successful occlusion (>80% drop from prestroke baseline). We injected 4.8 μg of the Exp pep or DM pep in 4 μL saline into the left lateral ventricle (anterior–posterior, −0.8 mm posterior; medial–lateral, 1.4 mm; and dorsal–ventral, −3.7 mm) of the rats immediately before the ischemia surgery. The infarct volume was determined 4 h later.

ACKNOWLEDGMENTS. We thank Dr. Kristen Johansen for fly strains. H.S. and M.J.W. are investigators of the Howard Hughes Medical Institute, at the Rockefeller University and University of Iowa. This work was supported by funding from the Chinese Ministry of Science and Technology (2013CB530700 and 2009CB941300) (to L.L.), the National Natural Science Foundation of China (NSFC31171324) (to L.L.), and the Peking-Tsinghua Center for Life Sciences (L.L.).

1. Syntichaki P, Tavernarakis N (2003) The biochemistry of neuronal necrosis: Rogue biology? *Nat Rev Neurosci* 4(8):672–684.
2. Yuan J, Lipinski M, Degterev A (2003) Diversity in the mechanisms of neuronal cell death. *Neuron* 40(2):401–413.
3. Moskowitz MA, Lo EH, Iadecola C (2010) The science of stroke: Mechanisms in search of treatments. *Neuron* 67(2):181–198.
4. Subramaniam S, Unsicker K (2010) ERK and cell death: ERK1/2 in neuronal death. *FEBS J* 277(1):22–29.
5. Wiegert JS, Bading H (2011) Activity-dependent calcium signaling and ERK-MAP kinases in neurons: A link to structural plasticity of the nucleus and gene transcription regulation. *Cell Calcium* 49(5):296–305.
6. Subramaniam S, et al. (2004) ERK activation promotes neuronal degeneration predominantly through plasma membrane damage and independently of caspase-3. *J Cell Biol* 165(3):357–369.
7. Qureshi IA, Mehler MF (2013) Epigenetic mechanisms governing the process of neurodegeneration. *Mol Aspects Med* 34(4):875–882.
8. Zong WX, Thompson CB (2006) Necrotic death as a cell fate. *Genes Dev* 20(1):1–15.
9. Galluzzi L, et al. (2011) Programmed necrosis from molecules to health and disease. *Int Rev Cell Mol Biol* 289:1–35.
10. Syntichaki P, Xu K, Driscoll M, Tavernarakis N (2002) Specific aspartyl and calpain proteases are required for neurodegeneration in C. elegans. *Nature* 419(6910):939–944.
11. Xu K, Tavernarakis N, Driscoll M (2001) Necrotic cell death in C. elegans requires the function of calreticulin and regulators of Ca(2+) release from the endoplasmic reticulum. *Neuron* 31(6):957–971.
12. Kohda K, Wang Y, Yuzaki M (2000) Mutation of a glutamate receptor motif reveals its role in gating and delta2 receptor channel properties. *Nat Neurosci* 3(4):315–322.
13. Yang Y, Hou L, Li Y, Ni J, Liu L (2013) Neuronal necrosis and spreading death in a Drosophila genetic model. *Cell Death Dis* 4:e723.
14. Clarke PG (1990) Developmental cell death: Morphological diversity and multiple mechanisms. *Anat Embryol (Berl)* 181(3):195–213.
15. Declercq W, Vanden Berghe T, Vandenabeele P (2009) RIP kinases at the crossroads of cell death and survival. *Cell* 138(2):229–232.
16. Shaukat Z, Wong HW, Nicolson S, Saint RB, Gregory SL (2012) A screen for selective killing of cells with chromosomal instability induced by a spindle checkpoint defect. *PLoS ONE* 7(10):e47447.
17. Morrison DK, Murakami MS, Cleghon V (2000) Protein kinases and phosphatases in the Drosophila genome. *J Cell Biol* 150(2):F57–F62.
18. Wang Y, Zhang W, Jin Y, Johansen J, Johansen KM (2001) The JIL-1 tandem kinase mediates histone H3 phosphorylation and is required for maintenance of chromatin structure in Drosophila. *Cell* 105(4):433–443.
19. Zhang W, et al. (2006) The JIL-1 histone H3S10 kinase regulates dimethyl H3K9 modifications and heterochromatic spreading in Drosophila. *Development* 133(2):229–235.
20. Gehani SS, et al. (2010) Polycomb group protein displacement and gene activation through MSK-dependent H3K27me3S28 phosphorylation. *Mol Cell* 39(6):886–900.
21. Fonseca JP, et al. (2012) In vivo Polycomb kinetics and mitotic chromatin binding distinguish stem cells from differentiated cells. *Genes Dev* 26(8):857–871.
22. Schuettengruber B, Martinez AM, Iovino N, Cavalli G (2011) Trithorax group proteins: Switching genes on and keeping them active. *Nat Rev Mol Cell Biol* 12(12):799–814.
23. Simon JA, Kingston RE (2009) Mechanisms of polycomb gene silencing: Knowns and unknowns. *Nat Rev Mol Cell Biol* 10(10):697–708.
24. Gindhart JG, Jr, Kaufman TC (1995) Identification of Polycomb and trithorax group responsive elements in the regulatory region of the Drosophila homeotic gene Sex combs reduced. *Genetics* 139(2):797–814.
25. Degterev A, et al. (2008) Identification of RIP1 kinase as a specific cellular target of necrostatins. *Nat Chem Biol* 4(5):313–321.
26. Cho IJ, Woo NR, Shin IC, Kim SG (2009) H89, an inhibitor of PKA and MSK, inhibits cyclic-AMP response element binding protein-mediated MAPK phosphatase-1 induction by lipopolysaccharide. *Inflamm Res* 58(12):863–872.
27. Deak M, Clifton AD, Lucocq LM, Alessi DR (1998) Mitogen- and stress-activated protein kinase-1 (MSK1) is directly activated by MAPK and SAPK2/p38, and may mediate activation of CREB. *EMBO J* 17(15):4426–4441.
28. Vicent GP, et al. (2006) Induction of progesterone target genes requires activation of Erk and Msk kinases and phosphorylation of histone H3. *Mol Cell* 24(3):367–381.
29. Wang H, et al. (2004) Role of histone H2A ubiquitination in Polycomb silencing. *Nature* 431(7010):873–878.
30. Wysocka J, et al. (2005) WDR5 associates with histone H3 methylated at K4 and is essential for H3 K4 methylation and vertebrate development. *Cell* 121(6):859–872.
31. Patel A, Vought VE, Dharmarajan V, Cosgrove MS (2008) A conserved arginine-containing motif crucial for the assembly and enzymatic activity of the mixed lineage leukemia protein-1 core complex. *J Biol Chem* 283(47):32162–32175.
32. Hardingham GE, Fukunaga Y, Bading H (2002) Extrasynaptic NMDARs oppose synaptic NMDARs by triggering CREB shut-off and cell death pathways. *Nat Neurosci* 5(5):405–414.
33. Yang G, et al. (1997) C57BL/6 strain is most susceptible to cerebral ischemia following bilateral common carotid occlusion among seven mouse strains: Selective neuronal death in the murine transient forebrain ischemia. *Brain Res* 752(1-2):209–218.
34. Xu Z, et al. (2012) The role of WDR5 in silencing human fetal globin gene expression. *Haematologica* 97(11):1632–1640.
35. Bevers MB, Neumar RW (2008) Mechanistic role of calpains in postischemic neurodegeneration. *J Cereb Blood Flow Metab* 28(4):655–673.
36. Taghibiglou C, et al. (2009) Role of NMDA receptor-dependent activation of SREBP1 in excitotoxic and ischemic neuronal injuries. *Nat Med* 15(12):1399–1406.
37. Dreyer EB, Zhang D, Lipton SA (1995) Transcriptional or translational inhibition blocks low dose NMDA-mediated cell death. *Neuroreport* 6(6):942–944.
38. Alessandrini A, Namura S, Moskowitz MA, Bonventre JV (1999) MEK1 protein kinase inhibition protects against damage resulting from focal cerebral ischemia. *Proc Natl Acad Sci USA* 96(22):12866–12869.
39. Park J, et al. (2013) RAS-MAPK-MSK1 pathway modulates ataxin 1 protein levels and toxicity in SCA1. *Nature* 498(7454):325–331.
40. Ray SK, Hogan EL, Banik NL (2003) Calpain in the pathophysiology of spinal cord injury: Neuroprotection with calpain inhibitors. *Brain Res Brain Res Rev* 42(2):169–185.
41. Abdouh M, et al. (2012) Bmi1 is down-regulated in the aging brain and displays antioxidant and protective activities in neurons. *PLoS ONE* 7(2):e31870.
42. Dhungana H, et al. (2013) Aging aggravates ischemic stroke-induced brain damage in mice with chronic peripheral infection. *Aging Cell* 12(5):842–850.
43. Sattler R, Tymianski M (2001) Molecular mechanisms of glutamate receptor-mediated excitotoxic neuronal cell death. *Mol Neurobiol* 24(1–3):107–129.
44. Ikonomidou C, Turski L (2002) Why did NMDA receptor antagonists fail clinical trials for stroke and traumatic brain injury? *Lancet Neurol* 1(6):383–386.
45. Cook DJ, Teves L, Tymianski M (2012) Treatment of stroke with a PSD-95 inhibitor in the gyrencephalic primate brain. *Nature* 483(7388):213–217.
46. O'Donnell ME, Tran L, Lam TI, Liu XB, Anderson SE (2004) Bumetanide inhibition of the blood-brain barrier Na-K-Cl cotransporter reduces edema formation in the rat middle cerebral artery occlusion model of stroke. *J Cereb Blood Flow Metab* 24(9):1046–1056.
47. Zuo XL, Wu P, Ji AM (2012) Nylon filament coated with paraffin for intraluminal permanent middle cerebral artery occlusion in rats. *Neurosci Lett* 519(1):42–46.